

THE EFFECTIVENESS OF ELECTRON BEAM MELTING FOR REMOVING IMPURITIES FROM TECHNOGENIC METAL MATERIALS

Martin Markov¹, Vladislava Stefanova², Katia Vutova¹

¹Institute of Electronics, Bulgarian Academy of Sciences
72 Tzarigradsko chaussee Blvd., Sofia 1784, Bulgaria

²University of Chemical Technology and Metallurgy
8 Kliment Ohridski Blvd., Sofia 1797, Bulgaria
E-mail: katia@van-computers.com

Received 09 July 2023

Accepted 10 December 2023

DOI: 10.59957/jctm.v59.i2.2024.22

ABSTRACT

Electron beam melting and vacuum refining (EBMR) is a modern metallurgical method that has proven advantages in terms of environmental sustainability and efficiency for recycling refractory and reactive metals and alloys with unique physical, chemical, and mechanical properties.

In this work, the effectiveness for removing impurities from technogenic molybdenum, titanium, and hafnium metals using EBMR method is investigated. The thermodynamic and kinetic process conditions and their influence on the possibility of impurities' removal from the studied technogenic materials are discussed. It has been established that there are no thermodynamic limitations for the removal of silicon, antimony, iron, aluminum, and copper impurities at EBMR of molybdenum and the maximal overall removal efficiency is 58 %. In the case of titanium technogenic material, the highest refining efficiency and maximal overall impurity removal level of 99.97 % and 100 % for some inclusions (such as Fe, Cu, Ta, and Cd) are achieved. The studies show that impurities (metallic and non-metallic) can be effectively removed from technogenic hafnium using single e-beam refining processing and the highest refining effectiveness is 52.21 %.

The obtained results allow formulating the conditions of the refining process aiming to obtain metal materials with high purity, better structures and properties and demonstrate high effectiveness of the EBMR method.

Keywords: refractory and reactive technogenic metals, electron beam melting and refining, refining effectiveness, microstructures, micro-hardness.

INTRODUCTION

The increasing demand for pure and high-quality metals in various industries has led to the development of new technologies for refining metals and alloys and recycling metallic technogenic materials. Hafnium, molybdenum, and titanium are three metals with unique properties that make them useful in different industries. Hafnium has a unique ability to absorb neutrons, which makes it useful in the nuclear reactors. Hafnium alloys have excellent resistance to oxidation and corrosion at high temperatures, making them ideal for use in nuclear equipment, shipbuilding, and space equipment [1, 2].

They are also used in various other applications such as thermoelectric converters, electric heaters, and chemical equipment. Molybdenum is a versatile metal used in various industries such as chemical industry, electronics, instrumentation in rockets and nuclear reactors. Its unique properties make it useful in metallurgy for creating high-temperature and corrosion-resistant alloys for various applications [3]. Titanium and its alloys are popular in aerospace, biomedical and chemical industries due to their light weight, heat resistance, high strength, fracture toughness, and corrosion resistance [4]. They are also used in other high-tech areas thanks to their low coefficient of thermal expansion and long fatigue

life [5]. However, production processes of pure metals (such as Hf, Mo, Ti, etc.) and their alloys can be costly, environmentally unfriendly, and result in impurities that reduce the quality of the produced metal ingots.

The requirements for the production of high-purity metals have led to the development and utilization of new methods such as electron beam drip melting and refining and electron beam cold hearth refining. These methods successfully compete with and even surpass conventional methods for metal refining such as vacuum induction melting, vacuum arc remelting, electroslag remelting, and plasma remelting in a cooled copper crucible [6 - 10]. At vacuum induction melting, the molten metal gets contaminated by the refractory materials of the pot and the gases adsorbed in it. These disadvantages are avoided in vacuum arc melting with fusible electrodes in a water-cooled copper crucible due to the intense cooling of the copper crucible [10]. However, this method does not provide the required metal purity for specific applications. Additionally, this method requires prior preparation of the electrodes and multiple material remelting.

Additive manufacturing (AM) is an advanced technique used for the manufacturing of near-net shape complex geometries and structure by adding material in layer form, using 3D model data. There are distinct AM techniques such as Electron Beam Selective Melting (EBSM), Selective Laser Melting (SLM), etc. [11 - 14]. Electron beam selective melting is a powder bed fusion technique and uses an electron beam as the power source to print 3D metal samples. Although AM has lot of advantages such as creation of complex shape, cheaper for small batch production, single step operation, etc. over traditional manufacturing, but still it has some limitations such as poor mechanical properties, limited materials availability, high cost for large volume production, etc.

EBMR method utilizes the kinetic energy of electrons to melt and refine metal materials, resulting in improved material quality and reduced impurity (inclusion) content [6, 15]. The combination of high vacuum conditions ($\sim 10^{-4}$ Pa) and heating of metal materials using an unconventional heating source (electron beam) makes the EBMR process highly effective even for the most refractory and chemically active metals at high temperatures such as hafnium, molybdenum, titanium, tungsten, tantalum, zirconium,

platinum, etc. and their alloys [16 - 18]. The use of vacuum enables to shift chemical interaction equilibria involving the gas phase. The application of the EBMR method provides a higher degree of refinement of metal materials by removing metallic and non-metallic inclusions (such as oxygen, hydrogen, and carbon). During the melting and crystallization processes, there is no contamination from the crucible material. The method enables the production of metal ingots with various sizes and shapes (from a few grams to tens of tons) with a homogeneous structure, free from defects, and improved working characteristics and properties.

The present work is a continuation of the studies carried out so far on the kinetics and mechanism of the removal of impurities from technogenic hafnium, molybdenum, and titanium scrap under EBMR conditions [19 - 21]. The purpose of this paper is a comparative analysis and evaluation of the effectiveness of single electron beam melting and refining of these refractory and reactive materials. The influence of melting power (heating temperature) and refining time on the removal efficiency, metal microstructure, and hardness is investigated and the obtained results provide insight into the possibility of using EBMR method for processing technogenic metal materials (Hf, Mo, and Ti) and obtaining pure metals.

EXPERIMENTAL

The ELIT-60 installation (Leybold GmbH, Germany, (Fig. 1) is used in the Laboratory "Physical problems of electron beam technologies" at the Institute of Electronics, Bulgarian Academy of Sciences for conducting experiments on EBMR. The melting and refining processes take place in a metal chamber, which is equipped with an electro-optical system (EOS) where the electron beam with a power of 60 kW is formed. The system also includes a mechanism for horizontal feeding of the input material, a copper water-cooled crucible with a movable bottom, and a device for extracting the formed pure metal specimen after electron beam processing [6].

Table 1 presents the elemental composition of the studied technogenic refractory and reactive metals - hafnium, molybdenum, and titanium prior to the electron beam refining. Accurate measurements of the contents of the base metal Hf and the controlled metallic and non-metallic impurities (such as Zr, Cr, Fe, Zn, [O], and C)

Table 1. Chemical composition of technogenic Hf, Mo, and Ti scrap before being treated by e-beam melting and refining (in mass. %).

Material	Sb	Si	Al	W	Cu	Fe	Mo	Ir	Ti	Hf	Zr	Cr	Others	Σ_{imp}
Hf	-	-	-	-	-	0.15	-	-	-	97.87	1.87	0.04	0.073***	2.13
Mo	2.0	1.0	0.5	0.2	0.08	0.03	95.59	-	-	-	-	-	0.60*	4.41
Ti	-	4.94	3.28	0.1	1.52	2.36	-	3.66	84.01	-	-	-	0.13**	15.99

*)0.3% Sn, 0.3% Ni; **)0.03% Ta, 0.1% Cd; ***)0.006% Zn, 0.032% [O], 0.035% C.



Fig. 1. External view of the ELIT-60 machine.

before and after single EBMR processing were obtained by ICP-OES, CS and ONH analyzers. To determine the chemical composition variation of Mo and Ti materials before and after e-beam processing, emission spectral analysis was conducted using UBI 1, Carl Zeiss, Jena, Germany.

It can be seen that the overall impurity content in technogenic hafnium is relatively low (2.13 %). However, the high content of Zr (87.8 % of the present impurities) is evident. It also contains non-metallic inclusions such as oxygen and carbon, indicating the presence of oxides and carbides. In the technogenic molybdenum, the highest contents are of Sb and Si, which account for 45.4 % and 22.7 % of the total impurity quantity, respectively. The Ti scrap exhibits the lowest purity (84.01 % Ti). The total impurity content is 15.99 %, with approximately 30.9 % Si, 20.5 % Al, 9.5 % Cu, 14.8 % Fe, and 22.9 % Ir, while the content of other impurities in the initial Ti is < 1 %.

The EBMR processing of the investigated technogenic material was performed using the ELIT-60 furnace under single refining at different process

conditions - e-beam melting power P_b (temperature of thermal treatment) and lengths of residence time (refining time). The operating process parameters at EBMR of the three wastes are given in Table 2.

The temperature was measured using a QP-31 optical pyrometer equipped with special correction filters for all three technogenic materials.

RESULTS AND DISCUSSION

Thermodynamic conditions of the evaporation processes during EBMR of technogenic hafnium, molybdenum, and titanium scrap

Since in the vacuum chamber the pressure is constant during the EBMR process, the refining process (impurities removal) is affected by the temperature of thermal treatment, the physical state (solid (s), liquid (l), or gaseous (g) state) of the inclusions, and the processes of mass transport of particles from the volume of the liquid metal pool to the reaction surface (liquid metal material/vacuum) [6].

Depending on the thermodynamic conditions of the melting process - the heat treatment temperature and the pressure in the vacuum chamber, the vapor pressures of metallic impurities and their compounds play a crucial role in the e-beam refining. The refining (component removal) could be realized through: (i) degassing - evaporation of inclusions (metallic or nonmetallic), which have vapor pressure (p_i) higher than the vapor pressure (p_R) of the base metal material ($p_i > p_R$) and the separated product is in gaseous final state; or through (ii) distillation - evaporation of more volatile compounds of the metal components.

The vapor pressure of the metal can be calculated from the evaporation reaction:

$$Me(s,l) = Me(g) \quad (1)$$

For pure metals, the activity ($a_{(Me)}$) is equal to 1 and thus the equilibrium constant K is equal to the vapor pressure of the specific metal ($p_{i(Me)}$):

Table 2. Process parameters at single EBMR of technogenic Hf, Mo, and Ti scrap.

Material	Specimen	Working vacuum pressure, Pa	Operating temperature, K (Pb, kW)	Refining time, min
Hf	Hf-01	1×10^{-3} Pa	2700 (15 kW)	5
	Hf-08			8
	Hf-10		2800 (16 kW)	5
	Hf-09			8
	Hf-05		2900 (17 kW)	5
	Hf-04			8
Mo	Mo-11	$5-8 \times 10^{-3}$ Pa	2900 (15 kW)	5
	Mo-12			10
	Mo-21		3000 (17 kW)	5
	Mo-22			10
Ti	Ti-02	$3-6 \times 10^{-3}$ Pa	1970 (2.5 kW)	25
	Ti-04			40
	Ti-03		2050 (3.5 kW)	25
	Ti-06			40
	Ti-07		2150 (5.5 kW)	25
	Ti-05			40

$$K = \frac{P_{i(M\epsilon)}}{a_{(M\epsilon)}} = P_{i(M\epsilon)} \quad (2)$$

In vacuum conditions, the equilibrium constant of the reaction of metal evaporation can be calculated from:

$$\ln p_{i(M\epsilon)} = -\frac{\Delta G}{R.T} \quad (3)$$

where ΔG is the Gibbs free energy, R is the gas constant, and T is the temperature (K). The values of ΔG vary with changes in pressure and temperature and are calculated using the equation:

$$\Delta G = \Delta G^{\circ} - RT \ln p^n \quad (4)$$

where ΔG° and ΔG are the free energies of the reactions occurring at atmospheric pressure and under vacuum conditions, respectively p , is the pressure at which the refining process takes place, and n is the number of atoms involved in the reaction.

The calculations were performed using the professional program for thermochemical calculations, HSC Chemistry ver.7.1 module "Reaction Equation" considering the physical state of the substances [22].

The melting and boiling temperatures as well as the density of the studied technogenic metal materials (Hf, Mo, and Ti) and the main metallic inclusions are shown in Fig. 2 and Fig. 3.

Considering the presence of metallic impurities (Zr, Cr, and Fe) in the technogenic hafnium and their melting temperatures, it can be seen that they will remain in a liquid state throughout the temperature range of EBM processing (2700 K - 2900 K) (Fig. 2). Furthermore, the densities of Zr, Cr, and Fe are significantly lower than that of hafnium, indicating that they can vaporize from the surface of the liquid pool (Fig. 3).

Molybdenum is characterized by a high melting temperature (2896 K, Fig. 2). Among the metallic impurities present in it, tungsten (W) has a higher melting temperature. It also has a much higher density (19300 kg m⁻³) compared to molybdenum (10200 kg m⁻³, Fig. 3). Therefore, during EBMR of Mo, tungsten will remain in a solid state and easily sink into the liquid pool. The other impurities present in the technogenic molybdenum such as Sb, Si, Al, Cu, and Fe, have significantly lower melting temperatures than that of the base metal and at the investigated working temperatures (2900 K - 3000 K) they will be in a liquid state. The

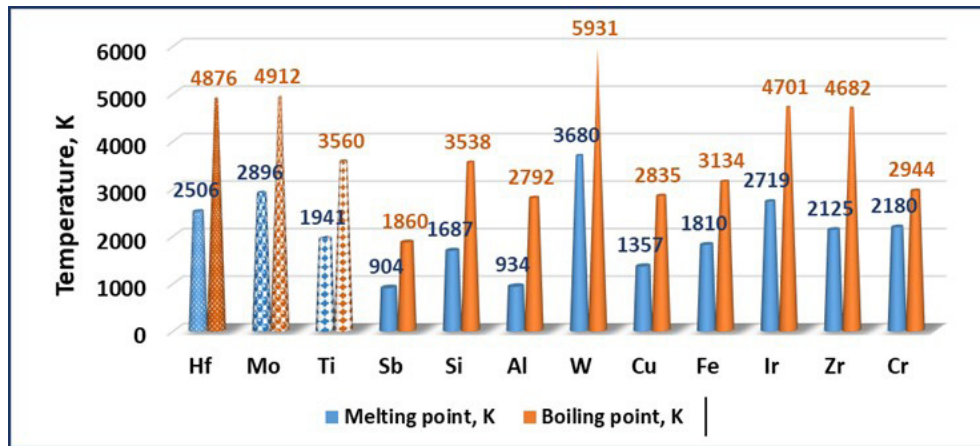


Fig. 2. The melting and boiling temperatures of the base metals and main metal inclusions present in them.

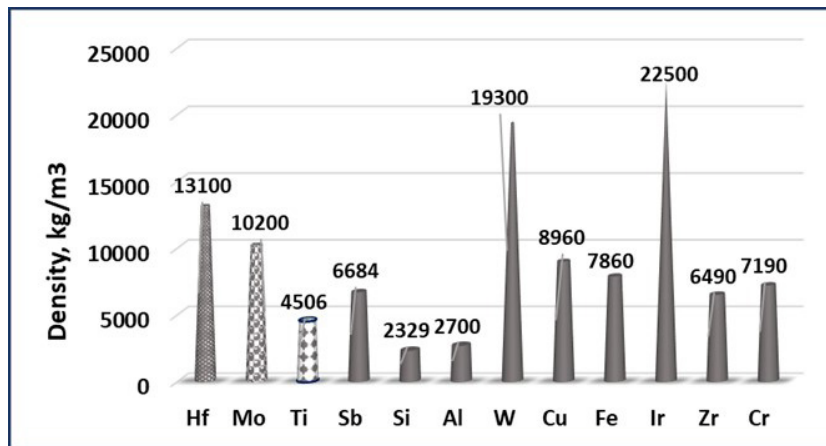


Fig. 3. The density values of the studied elements.

densities of these inclusions are considerably lower than that of molybdenum and during e-beam melting they will float to the surface of the liquid pool.

Among the impurities present in the Ti scrap, only Ir and W have significantly higher melting temperatures than that of Ti and therefore they will remain in a solid state at temperatures in the range of 1970 K to 2150 K. Fig. 3 shows that the densities of these two metals are much higher than that of Ti making it difficult for them to move and separate from the reaction surface.

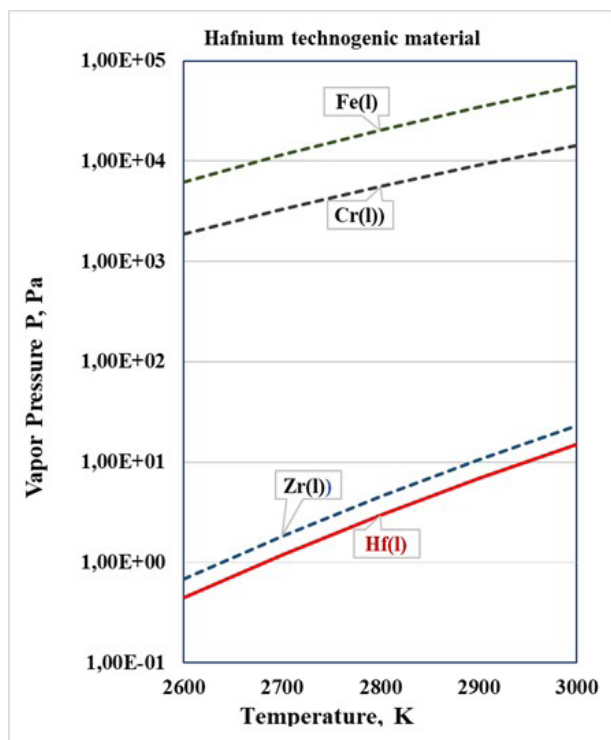
Fig. 4 presents the calculated values of the vapor pressure of the investigated technogenic materials and of the main controlled metallic inclusions under the studied EBMR processing conditions.

The obtained results indicate that the metal impurities Fe and Cr present in technogenic hafnium can be removed by evaporation at EBMR - their vapor pressure is significantly higher than that of Hf (Fig. 4(a)). The zirconium vapor pressure is slightly higher than that

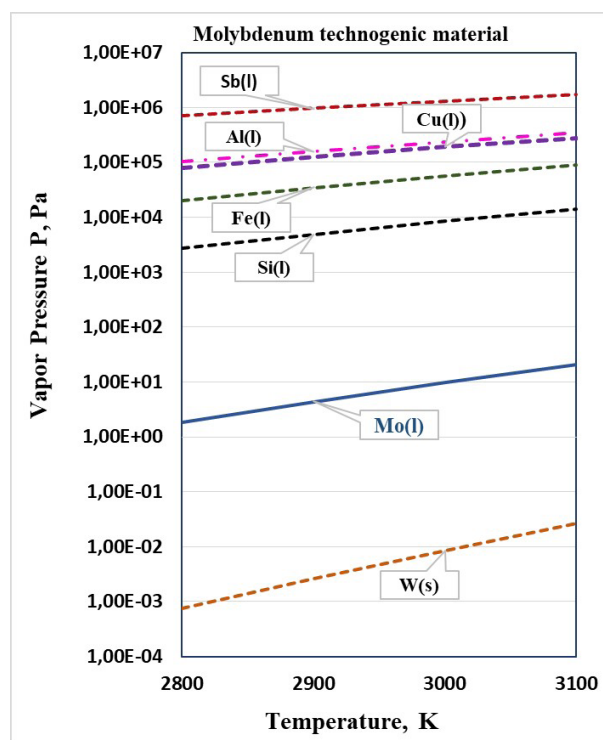
of Hf and therefore its evaporation is thermodynamically probable, but it will be accompanied by losses of hafnium (base metal).

Among all the impurities present in technogenic Mo only tungsten cannot be removed during the EBMR - its vapor pressure is lower than that of Mo. This is due to both the high melting temperature and high density of W. The other controlled impurities (such as Fe, Cu, Al, Si, and Sb) can be removed through degassing during the e-beam processing of Mo (Fig. 4(b)). Their partial pressure is several orders of magnitude higher than that of molybdenum.

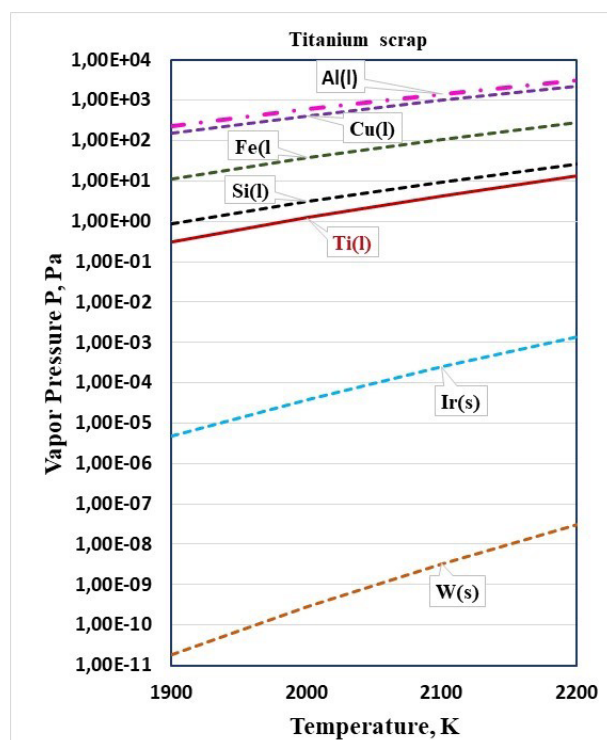
In the case of EBMR of the titanium scrap, it can be seen that vapor pressure of tungsten and iridium is much lower than that of titanium and their removal by evaporation is thermodynamically impossible (Fig. 4(c)). The results show that the vapor pressure of the other controlled inclusions such as Al, Cu, and Fe is higher than that of titanium and therefore they can



(a)



(b)



(c)

Fig. 4. The vapor pressure of: (a) technogenic hafnium; (b) molybdenum; (c) titanium scrap during EBMR for the investigated temperature ranges.

be removed by evaporation from the reactive surface (liquid metal/vacuum). The vapor pressure of silicon is slightly higher than that of titanium and its vaporization is thermodynamically possible, but will be accompanied by losses of the base metal (Fig. 4(c)).

To determine the relative efficiency for the elements' removal to the base metal (relative volatility) the following equation is used [23]:

$$\alpha_i = \frac{p_R}{p_i} \frac{\sqrt{M_i}}{\sqrt{M_R}} \quad (5)$$

where p_R and p_i are the vapor pressures of the base metal and of the metallic inclusion, respectively; M_R and M_i are the molecular masses of the base metal and of the metallic element, respectively.

The calculated values of the relative volatility α_i for the metallic impurities present in the technogenic Hf, Mo, and Ti scrap at the maximum operating temperatures are shown in Fig. 5. The value of the relative volatility of tungsten with respect to titanium is not included in the figure as it is very high ($> 10^8$) at a temperature of 2150 K. It can be seen that the parameter α_i varies widely depending on the type of metallic impurities present in the studied material. For hafnium, the values of α_i range from 10^{-5} to 10^0 ; for molybdenum, they vary from $\sim 10^{-6}$ to $\sim 10^4$; and for titanium, they range from $\sim 10^{-4}$ to $\sim 10^9$.

The analysis of the obtained results shows that $\alpha_i \ll 1$ for chromium and iron, i.e. both impurities can be easily separated from the base metal (Hf). The value of α_{Zr} is close to 1, but is situated on the left of Hf (is less than 1) and therefore the separation is thermodynamically probable

and accompanied by Hf losses.

The calculated values of α_i for the impurities present in molybdenum, except for W, are also $\ll 1$. Therefore, their volatilities with respect to molybdenum are high and can be arranged in the following sequence: $Sb > Al > Cu > Fe > Si$ and their removal is expected to be possible. The value of α_i for W is three orders of magnitude higher than that of molybdenum, indicating that its removal is not possible.

The α_i values for the inclusions present in Ti such as aluminum, copper, iron, and silicon are significantly lower than that of titanium and therefore their removal is expected to be effective and before the base metal. In contrast to these impurities, α_i for Ir and especially for W ($> 10^8$) is much higher than that of titanium, i.e. these metals cannot be removed from the titanium scrap at the maximum operating temperature (2150 K).

Refining effectiveness of impurities removal from technogenic Hf, Mo, and Ti scrap during EBMR

The total content of impurities in the material obtained under different EBMR technological regimes for the three metals is given in Table 3. The refining efficiency (β_{ref}) is determined by the following equation:

$$\beta_{ref} = \frac{C_{o,tot} - C_{r,tot}}{C_{o,tot}} 100 \% \quad (6)$$

where $C_{o,tot}$ and $C_{r,tot}$ are the overall concentrations of the all impurities in the initial technogenic material and in the metal specimen after refining, respectively.

The calculated values of the efficiency at single refining of the investigated technogenic materials (Hf,

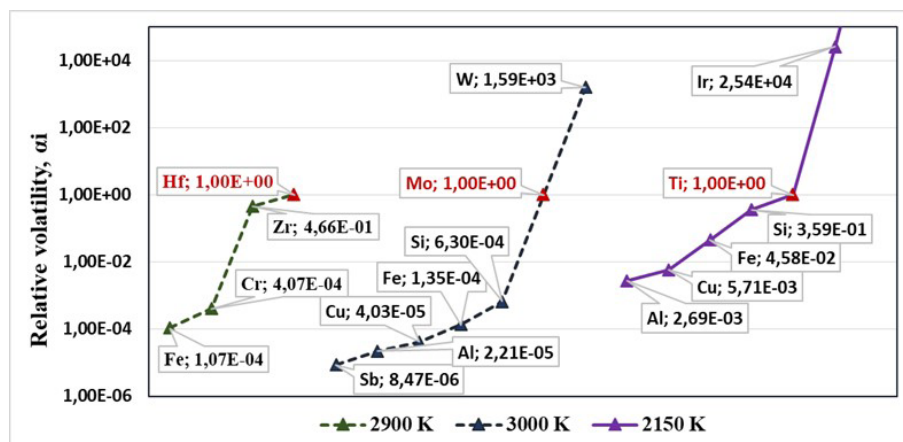


Fig. 5. Values of the relative volatility α_i for the metal impurities in technogenic hafnium, molybdenum, and titanium scrap at maximum working temperatures.

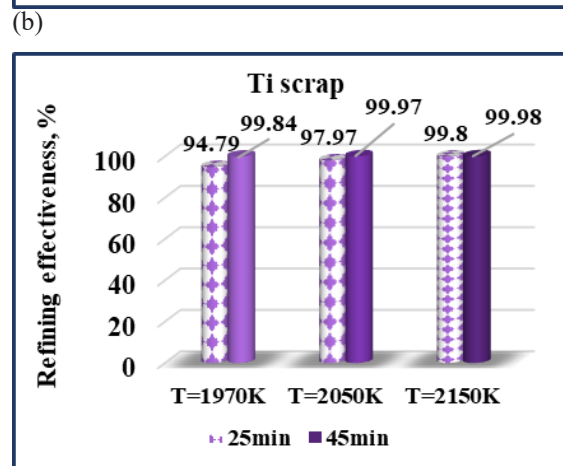
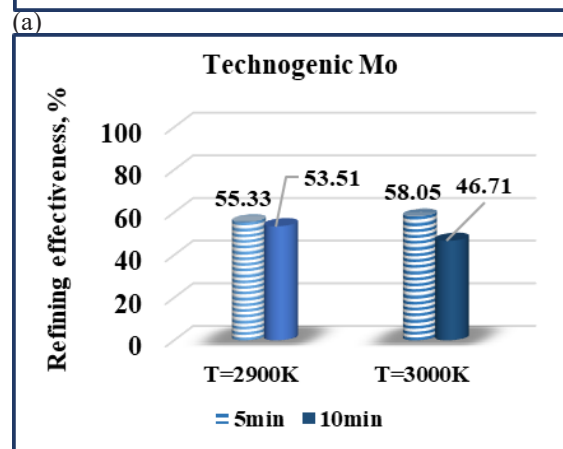
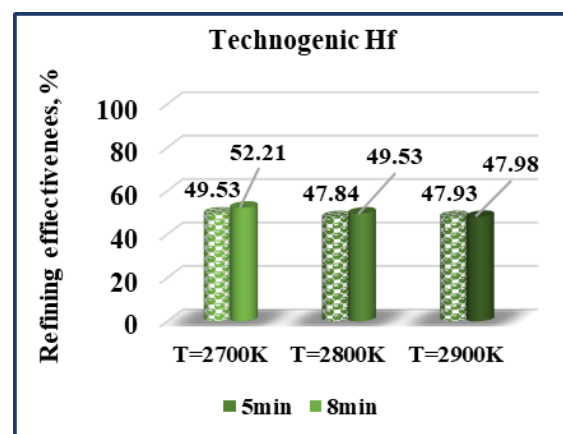
Table 3. Content of the impurities in the investigated materials after EBMR under different technological modes.

Specimen	Working temperature, K	Refining time, min	Σ_{imp} , %
Hf-01	2700	5	1.075
Hf-08		8	1.018
Hf-10	2800	5	1.111
Hf-09		8	1.075
Hf-05	2900	5	1.109
Hf-04		8	1.108
Technogenic hafnium before EBMR			2.13
Mo-11	2900	5	1.97
Mo-12		10	2.05
Mo-21	3000	5	1.85
Mo-22		10	2.35
Technogenic molybdenum before EBMR			4.41
Ti-02	1970	25	0.833
Ti-04		40	0.026
Ti-03	2050	25	0.336
Ti-06		40	0.005
Ti-07	2150	25	0.206
Ti-05		40	0.004
Titanium scrap before EBMR			15.99

Mo, and Ti scrap) under the conditions of EBMR are shown in Fig. 6.

The obtained results indicate that increasing the temperature does not lead to an increase in the efficiency of the refining process of technogenic hafnium. This can be explained by the high content of zirconium in the investigated material (~87.8 % of all present impurities). In our previous study [19], it was found that the maximum removal rate of Zr at single refining is 45.6 %. The best purification of technogenic hafnium was achieved at a temperature of heat treatment of 2700 K and a melting time of 8 min (Fig. 6(a)). These results confirm the significant similarity in the physical and chemical properties of Hf and Zr, which hinders their separation.

The results presented in Fig. 6(b) for molybdenum show that the evaluated values of the refining efficiency



(c) Fig. 6. Effect of the working temperature and residence time on the refining effectiveness of EBMR of: (a) technogenic Hf; (b) Mo; (c) Ti scrap.

at each EBMR regime range from 46.71 % to a maximum removal effectiveness of 58.05 %. The best refining effectiveness is achieved at temperature of 3000 K (17 kW) for a 5 min residence time and the highest molybdenum purity is 98.15 %.

The analysis of the calculated values for the refining effectiveness of titanium scrap shows that they are very high within the investigated temperature range (from 94.79 % to 99.97 %, Fig. 6(c)). It has been found that with the increase in the operating temperature (e-beam power) and refining time, the refining effectiveness increases [21]. The highest effectiveness of refining of 99.97 % is achieved at e-beam powers of 3.5 and 5.5 kW for 40 min (Fig. 6(c)).

Microstructures and micro-hardness of the investigated technogenic materials

It is known that the microstructure and mechanical properties of metals are strongly associated with their chemical composition and can vary significantly depending on the method of their production, cooling rate of the melts, impurity content, etc. The main factors that influence the microstructure at electron beam melting are the temperature gradient, solidification rate, content of inclusions, melting temperatures, etc. A high temperature gradient and low solidification rate result in planar grains in the solidification structure, while an increase in the solidification rate leads to equiaxed grains and dendrite structure.

Microstructure analysis of investigated materials was carried out using chemical etching with appropriate reagents: solution of 45 mL nitric acid, 45 mL water, and 10 mL hydrofluoric acid for Hf; solution of 68 % HNO₃, 98 % H₂SO₄, and water in proportion 1:1:1 for Mo; two reagents, including Kroll's reagent, prepared by mixing HF, HNO₃, and distilled water for Ti.

The microstructures of the etched surfaces of metal specimens were characterized using: a stereo microscope Leica M80 and a light microscope Leica DM2500 with a digital camera Leica EC3, and image processing software Leica LAS software, as well as a metallographic inverted microscope IM-3MET - Optika with a digital microscope camera Axiocam ERC5S-5MP. Microstructures of samples from initial technogenic materials Hf, Mo, and Ti and of specimens after EBMR at the highest process effectiveness are shown in Fig. 7.

On the micrograph of the initial technogenic hafnium (Fig. 7(a)), various colors and large polyhedral grains are observed. After EBMR of Hf, under the regime with the highest effectiveness of impurity removal, the structure of the obtained specimen is visibly changed (Fig. 7(b)). This is due to both the high removal rate of Fe and Cr

and the partial removal of Zr. The resulting structure is close-packing, fine-grained, and homogeneous. The grain shape approaches hexagonal with traces of solid solution between Zr and Hf along the grain boundaries.

The analysis of the microstructure of a sample from the initial technogenic molybdenum reveals a dendrite matrix with crystallized inhomogeneous molybdenum melts (Fig. 7(c)). The formation of different-colored phases is attributed to the formation of solid solutions and eutectic melts between Mo and other present metals inclusions (such as silicon, aluminum, antimony, etc.). After refining at $T = 3000$ K for 5 min, a body-centered cubic structure with an average grain diameter of ~ 100 μm is formed (Fig. 7(d)). This is attributed to the slow cooling of the ingot. Despite the presence of impurities (~ 1.8 %), the slow cooling process resulted in well-formed large grains.

The structure of the initial Ti scrap containing only 84.01 % Ti (Fig. 7(e)) is characterized by a disordered elongated type of structure which is a result of high impurities' content (Ir, Fe, Al, Cu, etc.) present in the material. After EBMR and the high degree of inclusions' removal, the resulting structure exhibits greater homogeneity and alignment, and is of the "basket-weave" type (Fig. 7(f)). The orientation of the lamellae is different due to the difference in the heat transfer rate in the melt volume.

One of the main mechanical characteristics of a given metal is its hardness, which is determined by the metal's structure. Therefore, it is of interest to compare the hardness of the initial materials with the hardness of the specimens obtained under the highest refining effectiveness. The measured micro-hardness values of the investigated samples, obtained using the Vickers method, are given in Table 4.

The analysis of the obtained results shows that the hardness of the specimens decreases after electron beam melting and impurities' removal. Analyzing the data reveals that the lowest micro-hardness of the Hf ingot (2378 MPa) is achieved after a single refining process at $T = 2700$ K for 8 min. The relative change in the hardness is 25 % compared to the initial material.

The biggest change in the hardness is observed in the ingot obtained after EBMR of technogenic molybdenum and the relative change of micro-hardness reaches 27 %. This decrease in hardness is attributed to both the high degree of impurity removal (~ 58 %) and the formation of a body-centered cubic structure.

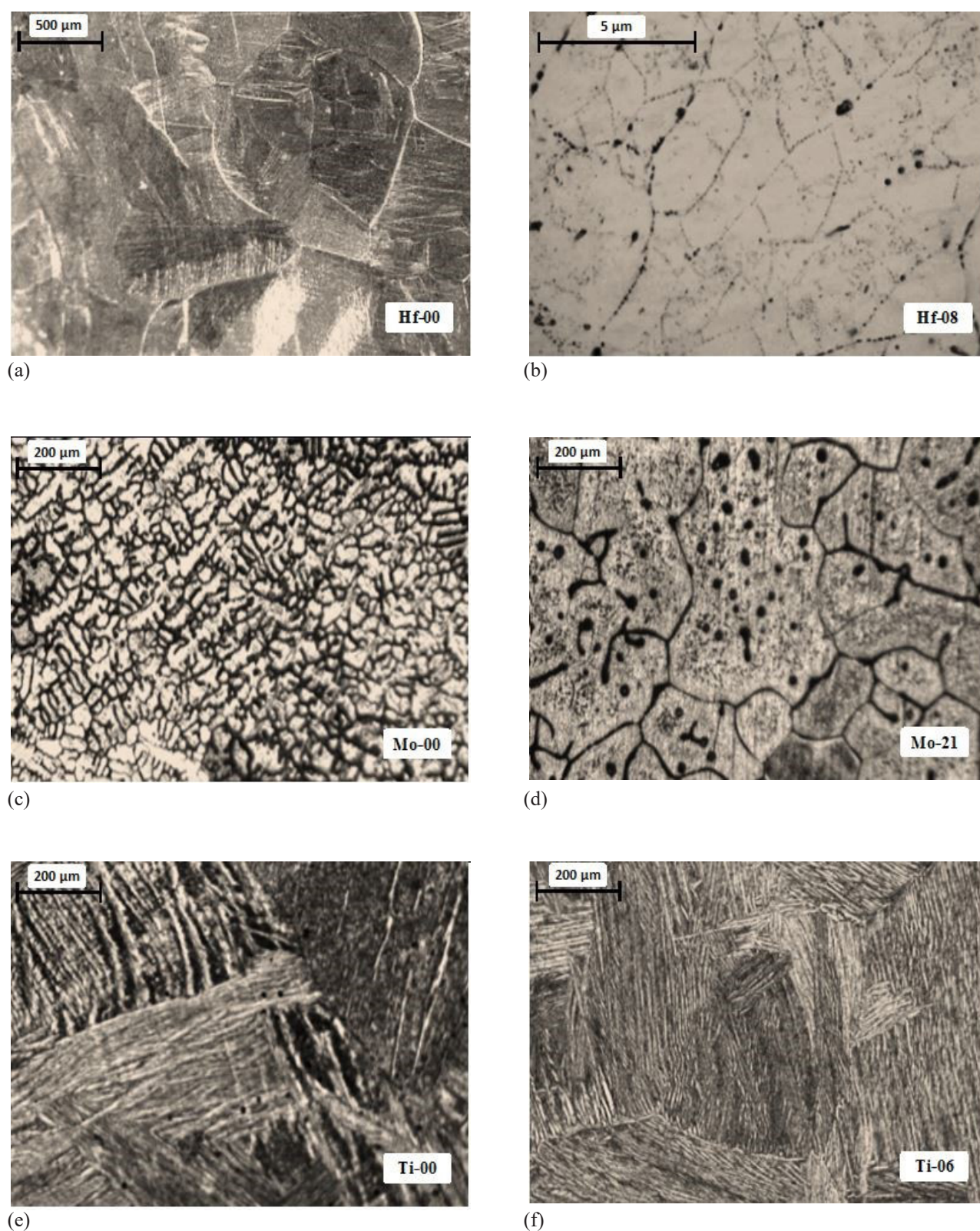


Fig. 7. Optical microphotographs of: technogenic Hf (500x magnification): (a) initial and (b) after EBMR at $T = 2700$ K for 8 min; technogenic Mo (100x magnification): (c) initial and (d) after EBMR at $T = 3000$ K for 5 min; Ti scrap (100x magnification); (e) initial and (f) after EBMR at $T = 2050$ K for 40 min.

Table 4. The average micro-hardness values before and after single EBMR and the relative changes of the micro-hardness values for technogenic Hf, Mo, and Ti scrap.

Material/ Probe	Micro-hardness MPa	Relative change of micro-hardness, %
Hf _{initial}	3166	25
Hf-08	2378	
Mo _{initial}	4066	27
Mo-21	2979	
Ti _{initial}	134	21
Ti-06	106	

In contrast to the molybdenum material, the relative change of micro-hardness in the titanium scrap is only 21 %, regardless of the high effectiveness of the refining process (> 99.9 %). The decrease in impurities' content (such as Fe, Si, Al, and Cu) and the formation of a "basket-weave" type structure cause the formation of a softer and more homogeneous material.

CONCLUSIONS

The influence of EBMR on the effectiveness of removal of inclusions from technogenic materials Hf, Mo, and Ti under different regimes (heating temperature and refining time) has been investigated and the following conclusions can be formulated:

- It has been found that the efficiency of metal element removal depends not only on the temperature and refining time but also on the physical state of the elements and their density.
- It has been demonstrated that under the investigated technological regimes of EBMR of technogenic Hf chromium and iron will be easily removed. The removal of zirconium is thermodynamically probable and is accompanied by Hf losses. In the case of technogenic Mo, the removal of tungsten is impossible, while the separation of other controlled metal inclusions is thermodynamically probable. Regarding the impurities present in titanium, except tungsten, the removal of iridium will also be significantly difficult.
- It has been shown that the effectiveness of impurity removal from the investigated technogenic materials depends on the type and quantity of inclusions present in the base metal, as well as the EBMR

parameters (working temperature, vacuum level, and refining duration). The maximum efficiency is the lowest for EBMR of technogenic Hf (52.21 %), which is attributed to the high content of zirconium (around 88 % of all present impurities). In the case of technogenic Mo, the maximum effectiveness is slightly higher (58.05 %) due to the presence of tungsten, which is difficult to separate under the investigated conditions (low degree of overheating of the base metal). The highest achieved efficiency (99.97 %) was obtained in refining Ti scrap, with a low tungsten content (0.6 % of all present inclusions).

- It was found that after EBMR processing of the studied technogenic materials, the metal specimens are with improved structures and their hardness decreases.

The obtained results indicate that the EBMR method is suitable for recycling technogenic materials containing refractory and reactive metals, to achieve high efficiency in impurity removal and improvement of the structure and mechanical properties of the resulting metals.

Acknowledgements

This work was supported by the Bulgarian Ministry of Education and Science under the National Research Programme "Young scientists and postdoctoral students - 2" approved by DCM 206/07.04.2022 (co-author MM) and by the Bulgarian National Science Fund under contract KP-06-N27/18 (co-author KV).

REFERENCES

1. A.K. Shikov, O.V. Bocharov, V.M. Arzhakova, V.N. Bezumov, Y.A. Perlovich, M.G. Isaenkova, Use of hafnium in control elements of nuclear reactors and power units, *Met. Sci. Heat Treat.*, 45, 2003, 300-303.
2. D. Sathiyamoorthy, S.M. Shetty, D.K. Bose, C.K. Gupta, Pyrochemical separation of zirconium and hafnium tetra-chlorides using fused salt extractive distillation process, *High Temp. Mater. Proc.*, 18, 4, 1999, 213-226.
3. H.J. Lunk, H. Hartl, Discovery, properties and applications of molybdenum and its compounds, *ChemTexts*, 3, 13, 2017, <https://doi.org/10.1007/s40828-017-0048-6>.
4. S. Gialanella, A. Malandrucolo, Titanium and titanium alloys, in: *Aerospace Alloys, Topics in Mining, Metallurgy and Materials Engineering*.

- Springer, Cham., 2020, https://doi.org/10.1007/978-3-030-24440-8_4.
5. C. Leyens, M. Peters, *Titanium and Titanium Alloys: Fundamentals and Applications*, Wiley-VCH Verlag GmbH & Co. KGaA, 2003, <https://doi.org/10.1002/3527602119>.
 6. G. Mladenov, E. Koleva, K. Vutova, V. Vassileva, in: M. Nemtanu, M. Brasoveanu (Eds.), *Practical Aspects and Application of Electron Beam Irradiation*, Transworld Research Network: Trivandrum, India, 2011, p. 43-93.
 7. L. Qianli, J. Peng, A. Feipeng, Design of crucible size of electron beam cold hearth melting for ultra-long and ultra-thin TC4 ingot, *Rare Metal Materials and Engineering*, 49, 5, 2020, 1476-1482.
 8. G. Kolobov, V. Pavlov, A. Karpenko, A. Kolobova, Refining refractory rare metals of group IV of the periodic table, *New materials and technologies in metallurgy and mechanical engineering*, 1, 2015, 89-95, (in Russian).
 9. E. Teke, M. Sütçü, Y. Baskurt, Ö. Seydibeyoglu, Recovery of pressed titanium alloy machining chip via vacuum induction melting, *Scientific Research Communications*, 2, 1, 2022, <https://doi.org/10.52460/src.2022.001>.
 10. J.M. Oh, J. Yang, J. Yoon, J.W. Lim, Effective method for preparing low-oxygen titanium ingot by combined powder deoxidation and vacuum arc melting processes, *Korean Journal of Metals and Materials*, 59, 3, 2021, 149-154.
 11. V.V. Popov, M.L. Grilli, A. Koptyug, Powder bed fusion additive manufacturing using critical raw materials: a review, *Materials*, 14, 909, 2021, 1-37, <https://doi.org/10.3390/ma14040909>.
 12. H. Yue, H. Peng, R. Li, R. Gao, X. Wang, Y. Chen, High-temperature microstructure stability and fracture toughness of TiAl alloy prepared via electron beam smelting and selective electron beam melting, *Intermetallics*, 2021, <https://doi.org/10.1016/j.intermet.2021.107259>.
 13. E. Sharabian, M. Leary, D. Fraser, S. Gulizia, Electron beam powder bed fusion of copper components: a review of mechanical properties and research opportunities, *Int. J. Adv. Manuf. Technol.*, 2022, <https://doi.org/10.1007/s00170-022-09922-6>.
 14. Y. Gui, K. Aoyagi, H. Bian, A. Chiba, Detection, classification and prediction of internal defects from surface morphology data of metal parts fabricated by powder bed fusion type additive manufacturing using an electron beam, *Additive Manufacturing*, 54, 102736, 2022, <https://doi.org/10.1016/j.addma.2022.102736>.
 15. R. Bakish, *Electron beam melting 1995 to 2005*, Proceedings of the 7th International Conference Electron Beam Technologies, Varna, 2003, 233-240.
 16. B.E. Paton, N.P. Trigub, S.V. Akhonin, Electron-beam melting of refractory and high-reactive metals, *Naukova Dumka*, 312, 2008, Kyiv, (in Russian).
 17. A. Gupta, B. Mishra, Tantalum recovery technique for recycling of tantalum coated composite materials. in: , et al. *Rare Metal Technology 2023*, TMS 2023, The Minerals, Metals & Materials Series, Springer, Cham. https://doi.org/10.1007/978-3-031-22761-5_25.
 18. N.I. Grechanyuk, P.P. Kucherenko, A.G. Mel'nik, I.N. Grechanyuk, Yu.A. Smashnyuk, Industrial electron-beam installation L-4 for melting and vacuum refining of metals and alloys, *Powder Metall Met Ceram* 55, 2016, 489-495, <https://doi.org/10.1007/s11106-016-9831-y>.
 19. K. Vutova, V. Stefanova, M. Markov, V. Vassileva, Study of the possibility of recycling of technogenic hafnium during electron beam refining, *Materials*, 15, 8518, 2022, <https://doi.org/10.3390/ma15238518>.
 20. K. Vutova, V. Vassileva, V. Stefanova, M. Naplatanova, Influence of process parameters on the metal quality at electron beam melting of molybdenum, *The Minerals, Metals & Materials Society*, 2020, https://doi.org/10.1007/978-3-030-36540-0_84.
 21. K. Vutova, V. Vassileva, V. Stefanova, D. Amalnerkar, T. Tanaka, Effect of electron beam method on processing of titanium technogenic material, *Metals*, 9, 683, 2019, <https://doi.org/10.3390/met9060683>.
 22. HSC Chemistry ver.7.1, Outotec, Research Center Pori, Finland, 2013, Available online: <http://www.hsc.chemistry.net/>.
 23. U.P. Bobrov, V.D. Virich, A.E. Dmitrenko, D.V. Koblik, G.P. Kovtun, V.V. Manjos, N.N. Pilipenko, I.G. Tancura, A.P. Shterban, Refining of ruthenium by electron beam melting. Questions of atomic science and technology: Vacuum, pure materials, superconductors, 6, 19, 2011, 11-17, (in Russian).